Available online at www.sciencedirect.com

jmr&t Journal of Materials Research and Technology

www.jmrt.com.br

Original Article

Effect of ceramic particulate type on microstructure and properties of copper matrix composites synthesized by friction stir processing

Issac Dinaharan[a], *Ramasamy Sathiskumar*[b,*], *Nadarajan Murugan*[b]

[a] *Department of Mechanical Engineering Science, University of Johannesburg, Auckland Park Kingsway Campus, Johannesburg, South Africa*

[b] *Department of Mechanical Engineering, Coimbatore Institute of Technology, Coimbatore, India*

ARTICLE INFO

Article history:
Received 14 November 2015
Accepted 18 January 2016
Available online 14 April 2016

Keywords:
Copper matrix composites
Friction stir processing
Microstructure
Wear

ABSTRACT

Friction stir processing (FSP) has been established as a novel solid state technique to produce bulk and surface metal matrix composites. The present work aim to produce copper matrix composites (CMCs) using FSP and analyze the effect of ceramic reinforcement type (SiC, Al_2O_3, B_4C and TiC) on the evolving microstructure, microhardness and wear resistance behavior. A groove was made on 6 mm thick copper plates and packed with various ceramic particles. A single pass FSP was carried out using a tool rotational speed of 1000 rpm, travel speed of 40 mm/min and an axial force of 10 kN. The microstructure and distribution of the ceramic particles were studied using optical and field emission scanning electron microscopy. The sliding wear behavior was evaluated using a pin-on-disk apparatus. The results indicate that the variation in the stir zone, distribution, grain size, hardness and wear resistance of CMCs were within a short range. Nevertheless, Cu/B_4C CMC exhibited superior hardness and wear resistance compared to other CMCs produced in this work under the same set of experimental conditions.

1. Introduction

The advancement of electronic and electrical industries has invoked a demand for high strength, high wear resistance and high conductivity connector materials. Pure copper is extensively used in those industries due to high electrical and thermal conductivity, formability and corrosion resistance [1–3]. However, the low wear resistance of pure copper places some limitations, especially for sliding applications. Copper matrix composites (CMCs) reinforced with ceramic particulates were developed to overcome the limitations [4,5]. CMCs are currently produced using powder metallurgy [6] and various casting routes [7–9]. It is extremely difficult to obtain a high performance CMCs due to porosity formation, interface debonding, poor distribution, low wettability and interfacial

* *Corresponding author.*
E-mail: sathiscit2011@gmail.com (R. Sathiskumar).

http://dx.doi.org/10.1016/j.jmrt.2016.01.003

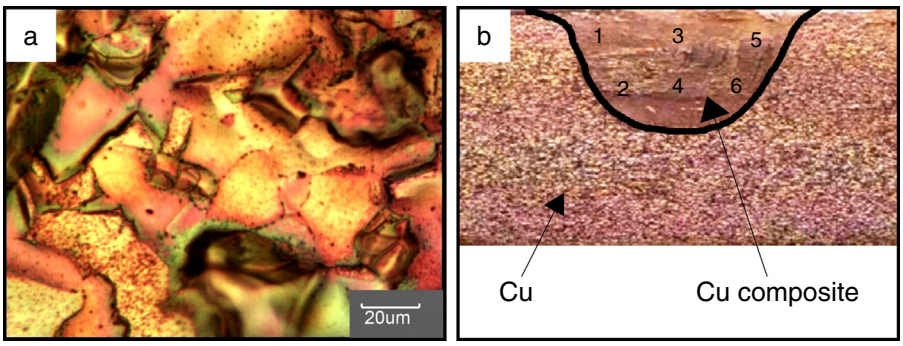

Fig. 1 – (a) Optical photomicrograph of pure copper and (b) location in stir zone to record the microstructure of CMCs.

reaction. Friction stir processing (FSP) is emerging as a promising technique to produce sound CMCs [10].

FSP is a novel solid state technique to fabricate bulk and surface metal matrix composites [11]. Mishra et al. [12] derived FSP based on the principles of friction stir welding (FSW) to synthesize metal matrix composites (MMCs). A groove of required width and depth [13] or a hole of required diameter and depth [14] is machined on the metallic plate to be processed. The chosen ceramic particles are subsequently compacted in the groove or the hole. A rotating tool under adequate axial force is plunged at one end and traversed along the groove or holes. The material undergoes severe plastic deformation during FSP which is utilized to form MMCs. FSP technique has been successfully explored by many investigators to fabricate aluminum [15], magnesium [16], copper [17], steel [18] and titanium [19] composites.

Some studies on CMCs reinforced with various ceramic particles produced using FSP were reported in literatures [20–30]. Barmouz et al. [20–22] produced Cu/SiC CMCs and studied the properties in detail. He observed that the traverse speed considerably influenced the distribution of SiC particle in the CMC [20]. The increase in volume fraction and decrease in the size of the SiC particle enhanced the tensile and wear properties of the CMC [21]. The increase in the number of passes during FSP improved the distribution of SiC particles and reduced the grain size [22]. Sarmadi et al. [23] prepared Cu/graphite CMCs and reported the influence of tool pin profile on microstructure and wear behavior. Sathiskumar et al. [24] fabricated

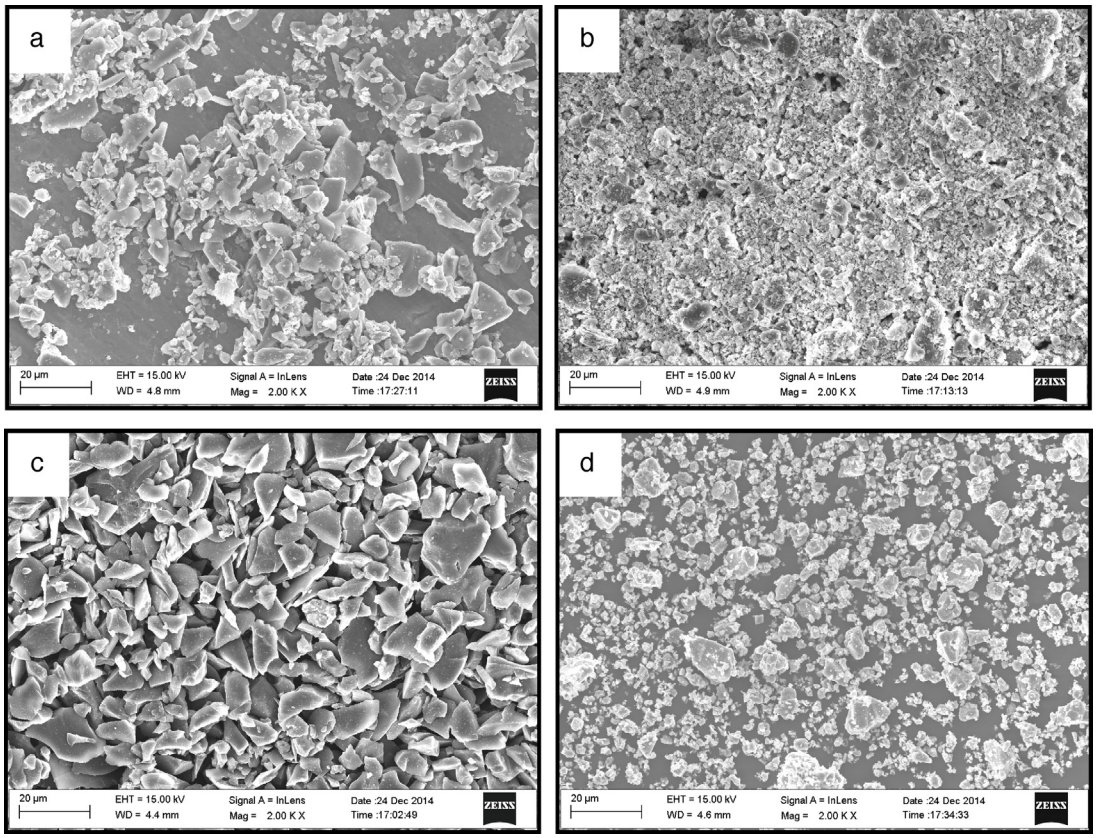

Fig. 2 – FESEM micrograph of ceramic particles: (a) SiC, (b) Al_2O_3, (c) B_4C and (d) TiC.

Cu/B_4C CMCs and investigated the effect of B_4C particle and its volume fraction on microstructure and wear behavior. Sathiskumar et al. [25] developed empirical relationships to predict the influence of process parameters on mechanical and wear properties of CMCs reinforced with SiC, Al_2O_3, B_4C, TiC and WC particulates. Akramifard et al. [26] synthesized Cu/SiC CMCs and showed that the SiC particles improved the mechanical and wear properties. Fenoel et al. [27] formed Cu/Y_2O_3 CMCs and demonstrated that the Y_2O_3 particles were effective to boost the mechanical properties. Khosravi et al. [28] developed Cu/WC CMCs and investigated the influence of number of passes on microstructure, mechanical and thermo physical properties. It was found that WC particles improved the mechanical properties and refined the grains of copper. Sabbaghian et al. [29] produced Cu/TiC CMCs using FSP and observed fine grains with a homogeneous distribution of TiC particles. Raju and Kumar [30] fabricated Cu/Al_2O_3 CMCs using FSP and analyzed the influence of process parameters on the tensile strength.

It has been demonstrated in literatures that it is feasible to produce CMCs reinforced with various ceramic particulates such as SiC, Al_2O_3, Y_2O_3, B_4C, TiC and WC. Multiple reinforcements were not compared in a single study which would help to evaluate the performance of various potential reinforcements under a set of similar experimental conditions. Hence, the objective of this research work is to produce CMCs reinforced with SiC, Al_2O_3, B_4C and TiC and evaluate the effect of various reinforcements on microstructure and sliding wear behavior. Silicon carbide (SiC) and alumina (Al_2O_3) are commonly used reinforcements for making CMCs, while boron carbide (B_4C) and titanium carbide (TiC) are used for specific applications [31–33].

2. Experimental procedure

Commercially available pure copper plates of 100 mm length, 50 mm width and 6 mm thickness were used in this research work. The optical photomicrograph of the as-received copper plate is shown in Fig. 1a. A groove of 2.5 mm deep and 0.7 mm width was made in the middle of the plate using wire EDM and compacted with ceramic particles. The volume fraction of ceramic particles was 12%. The SEM micrographs of as received ceramic particles are shown in Fig. 2. A pinless tool was initially employed to cover the top of the groove after filling with ceramic particles to prevent the particles from scattering during FSP. A tool made of double tempered hot working steel was used in this study [25]. The tool had a shoulder diameter of 20 mm, pin diameter of 5 mm and pin length of 3 mm. The FSP was carried out on an indigenously built FSW machine. The process parameters employed were tool rotational speed of 1000 rpm, travel speed of 40 mm/min and axial force of 10 kN. This set of process parameters was selected after trail experiments. Some of the defects encountered during trial experiments are shown in Fig. 3. Four such plates were friction stir processed by varying the ceramic particles (SiC, Al_2O_3, B_4C and TiC). A detailed FSP procedure to produce the composite is presented elsewhere [20].

Specimens were obtained from the center of the friction stir processed plates and were polished as per standard metallographic procedure. The polished specimens were etched with a color etchant containing 20 g chromic acid, 2 g sodium sulfate, 1.7 ml HCl (35%) in 100 ml distilled water. The digital image of the macrostructure of the etched specimens was captured using a digital optical scanner. The microstructure was observed using an optical microscope (OLYMPUS-BX51M) at various locations in the stir zone as indicated in Fig. 1b. The ceramic particle distribution was further viewed using a field emission scanning electron microscope (FESEM, CARL ZEISS-SIGMA HV). Energy dispersive spectroscope (EDS) attached to the FESEM was used to study the elemental distribution within the composite. The microhardness was measured using a microhardness tester (MITUTOYO-MVK-H1) at 500 g load applied for 15 s at various locations in the surface composite.

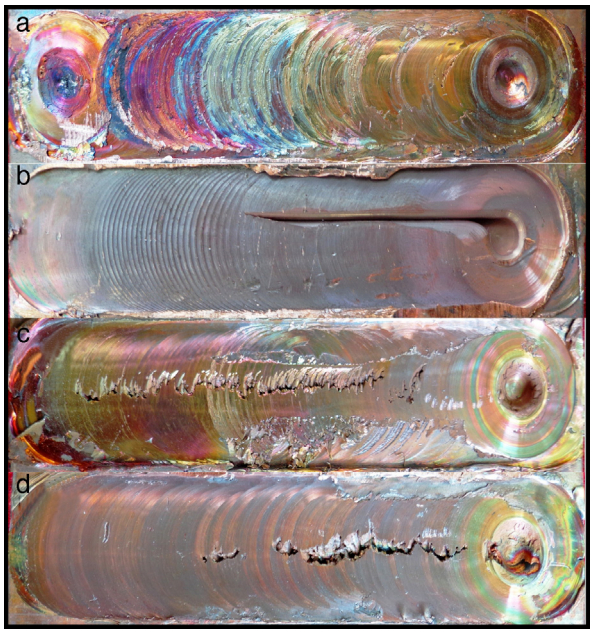

Fig. 3 – Typical defects appeared in trial specimens: (a) rough surface induced by insufficient plastic flow, (b) tool dragging, (c) incomplete bonding and (d) cracks.

The sliding wear behavior of Cu/X (X = SiC, Al_2O_3, B_4C and TiC) CMCs was measured using a pin-on-disk wear apparatus (DUCOM TR20-LE) at room temperature according to ASTM G99-04a standard. Specimens of size 3 mm × 5 mm × 20 mm were prepared from the FSP zone by wire EDM. The wear test was conducted at a sliding velocity of 1.5 m/s, normal force of 30 N and sliding distance of 3000 m. The polished surface of the pin was slid on a hardened chromium steel disk. A computer aided data acquisition system was used to monitor the loss of height. The volumetric loss was computed by multiplying the cross sectional area of the test pin with its loss of height. The wear rate was obtained by dividing volumetric loss to sliding distance. The worn surfaces of the test specimens were observed using the SEM. The wear debris, which were scattered on the face of the counterface, were carefully collected and characterized using SEM.

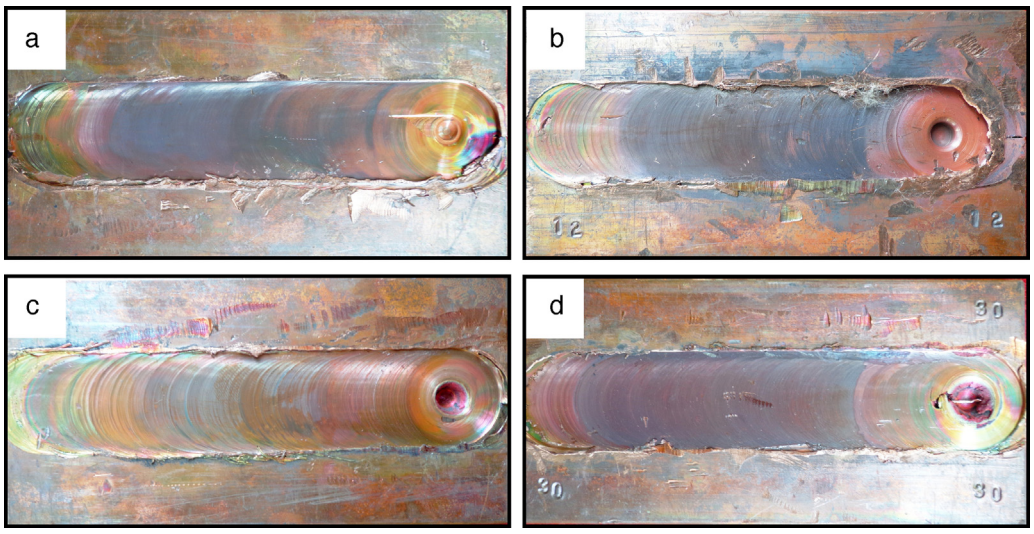

Fig. 4 – Crown appearance of CMCs reinforced with: (a) SiC, (b) Al_2O_3, (c) B_4C and (d) TiC.

3. Results and discussion

The crown appearance is an indication of the integrity of the stir zone underneath it. Any defect on the crown usually accompanies a corresponding defect in the stir zone. The crown appearances of friction stir processed copper with various ceramic particles are presented in Fig. 4. The surface of the crown is smooth without any depressions or discontinuities. A similar crown surface was observed irrespective of the type of ceramic particle used. Semicircular striations analogous to those generated in the conventional milling process are also visible on the crown. The optimized process parameters were carefully chosen to yield a defect free crown surface. The defects in the crown as revealed in Fig. 3 during trail runs can be attributed to poor material flow between advancing and retreading side and inadequate plasticization of copper.

3.1. *Macrostructure of CMCs*

Fig. 5 depicts the macrostructure of CMCs reinforced with various ceramic particles. The stir zone area which contains the CMC is clearly visible in all the figures. The marks of a groove made before FSP are not seen. It indicates the complete formation of the composite and continuous flow of plasticized material during FSP. The frictional heat generated by the rubbing of tool shoulder and the shearing of the pin plasticizes the copper matrix around and below the tool. The rotating and translation motion of the tool transports the plasticized copper from advancing side to retreading side. This material flow initially causes the groove to collapse and mixes the compacted ceramic particles with the plasticized copper. The rate at which the tool rotates and translates determines the intensity of mixing leading to the formation of the composite. The figure reveals that all kinds of ceramic particles mixed with the plasticized copper and formed the CMC. It can lead to a conclusion that the type of ceramic particle has no influence on the formation of composite during the FSP process. The boundaries of the stir zone are marked with black color. It is interesting that the boundaries are clearly visible on both the sides of the stir zone. Some researchers reported the absence of a clear boundary between the stir zone and the matrix material on the retreading side during FSW [34,35]. This could be due to inadequate forging at the back of the tool or excessive plasticization of the matrix. The measured values of the FSP area are furnished in Table 1. The size variation of the FSP area across the various ceramic particles is negligible. Under a set of FSP parameters, the variation in the flow stress of the material will cause variation in the size of the FSP zone. It is a well known fact that the addition of ceramic particle leads to the increase in flow stress [36]. The results demonstrate that the variation in flow stress of the copper by the reinforcement of different ceramic particles is negligible. Hence, there is no significant change in stir zone size.

It is evident from the figure that the stir zone of all CMCs is symmetric about the tool axis. A symmetric stir zone will have a homogeneous distribution of ceramic particles across the zone. The combination of tool rotation and translation tends to induce an asymmetric material flow in FSP [37]. Higher level of stirring in the advancing side will alter the symmetry of the stir zone. The formation of the symmetric stir zone can be attributed to even stirring and material transportation from advancing to retreading side. As a manufacturing process, FSP has its own defects such as pin holes, tunnels, voids, cracks and kissing bonds. Defects reduce the area of the stir zone and cause the composite susceptible to sliding wear and tensile loading. None of those defects appeared in the stir zone. The stir zone is completely defect free and sound. Defects arise due to several factors which is not limited to inadequate heat generation, material flow and consolidation. The process parameters govern those factors to a large extend. Absence of defects can be related to optimized process parameters employed in this work. It is worth mentioning that no onion rings characterized by arc lines typically seen in the stir zone of friction stir welded or processed monolithic alloys are not observed. This particular result agrees with the

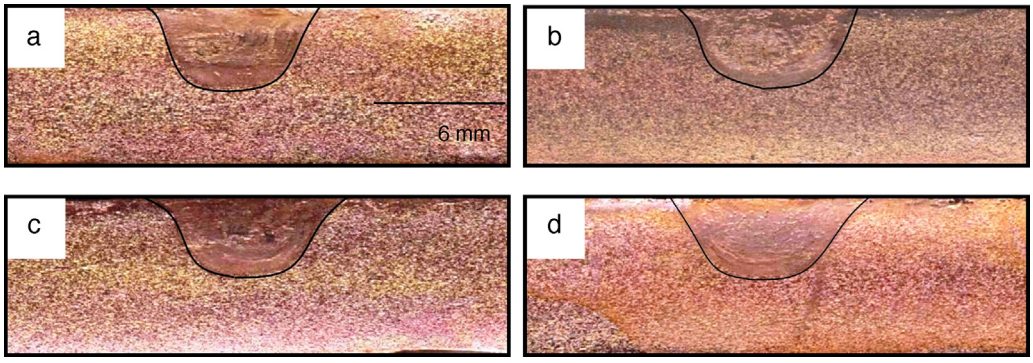

Fig. 5 – Macrostructure of CMCs reinforced with: (a) SiC, (b) Al_2O_3, (c) B_4C and (d) TiC.

findings of some earlier works on CMCs using FSP [20,21,23]. The amalgamation of material flow induced separately by the tool shoulder and tool pin produces alternative layers of high and low volume fraction of ceramic particles due to the temperature gradient along the depth of the welded plate [37]. The depth of penetration of the tool is not equal to the depth of total plate thickness in the production of composites by FSP. The absence of onion rings points out that the thermal gradient along the depth of the tool pin penetration is negligible. Because, the fixture made of different material acts as a backup plate in a conventional FSW. But, the same matrix material beyond the depth of tool penetration to the full thickness of plate serves as a back plate in FSP. Hence, the thermal gradient is insufficient to aid the formation of onion rings.

3.2. *Microstructure of CMCs*

Figs. 6–9 depict the optical micrographs of CMCs reinforced with various ceramic particles recorded at locations as marked in Fig. 1b. The optical micrographs reveal the distribution of ceramic particles all over the stir zone. No area in the stir zone is particle free. It is remarkable to observe that the distribution of the ceramic particle is independent of the location in the stir zone. The variation in the distribution of the ceramic particles from the advancing side to the retreading side or from the top side to the bottom side is infinitesimal. But researchers found significant variation in the distribution of ceramic particles within the stir zone of aluminum and magnesium composites synthesized by FSP [38–40]. This can be attributed to the material behavior of copper under frictional heat. The flow stress of copper is considerable higher to that of aluminum and magnesium which makes plasticization of copper little difficult. The plasticized copper will not flow easily compared to aluminum or magnesium. This provides more time for the ceramic particles to be well distributed within the plasticized copper before forging completes the formation of stir zone. Hence, the distribution of ceramic particles is superior to that of aluminum or magnesium composites.

It can be inferred from Figs. 6–9 that the type of ceramic particle does not play a major role to govern the nature of distribution in the composite. All the ceramic particles considered in this study combined well with the plasticized copper and produced the composite. This can be related to the nature of the FSP process, which forms the composite in solid state without melting the copper. Neither the density gradient nor the wettability between the type of ceramic particle and the copper causes uneven microstructure. It is very hard to produce CMCs reinforced with various ceramic particles using liquid metallurgy routes. The density gradient will cause the ceramic particle either to float or sink while poor wettability will result in the rejection of particles from the copper melt. FSP process is suitable and capable of producing CMCs reinforced with different ceramic particles.

The optical micrographs in Figs. 6–9 further shows the presence of finer grains compared to the grain size of copper in Fig. 1a. The average grain size is quantitatively presented in Table 1. The grain boundaries are not visible completely, but constructed using an image analyzing software for measurement [24]. The reinforcement of ceramic particles and the severe plastic deformation refined the grains of copper matrix. But the grain size across different CMCs is negligible. The following factors predominantly contribute to the grain refinement. FSP imposes severe plastic deformation, which leads to high dynamic stress as well as nucleation and increase in dislocation density. The movement of grain boundaries and subsequently the grain growth is prevented.

Table 1 – Properties of copper matrix composites.

Material	FSP area (mm^2)	Average grain size (μm)	Microhardness (VHN)	Wear rate (mm^3/m)
Cu	–	35	75	385
Cu/SiC CMC	39	6	116	245
Cu/Al_2O_3 CMC	40	3	119	231
Cu/B_4C CMC	37	5	135	213
Cu/TiC CMC	42	4	126	225

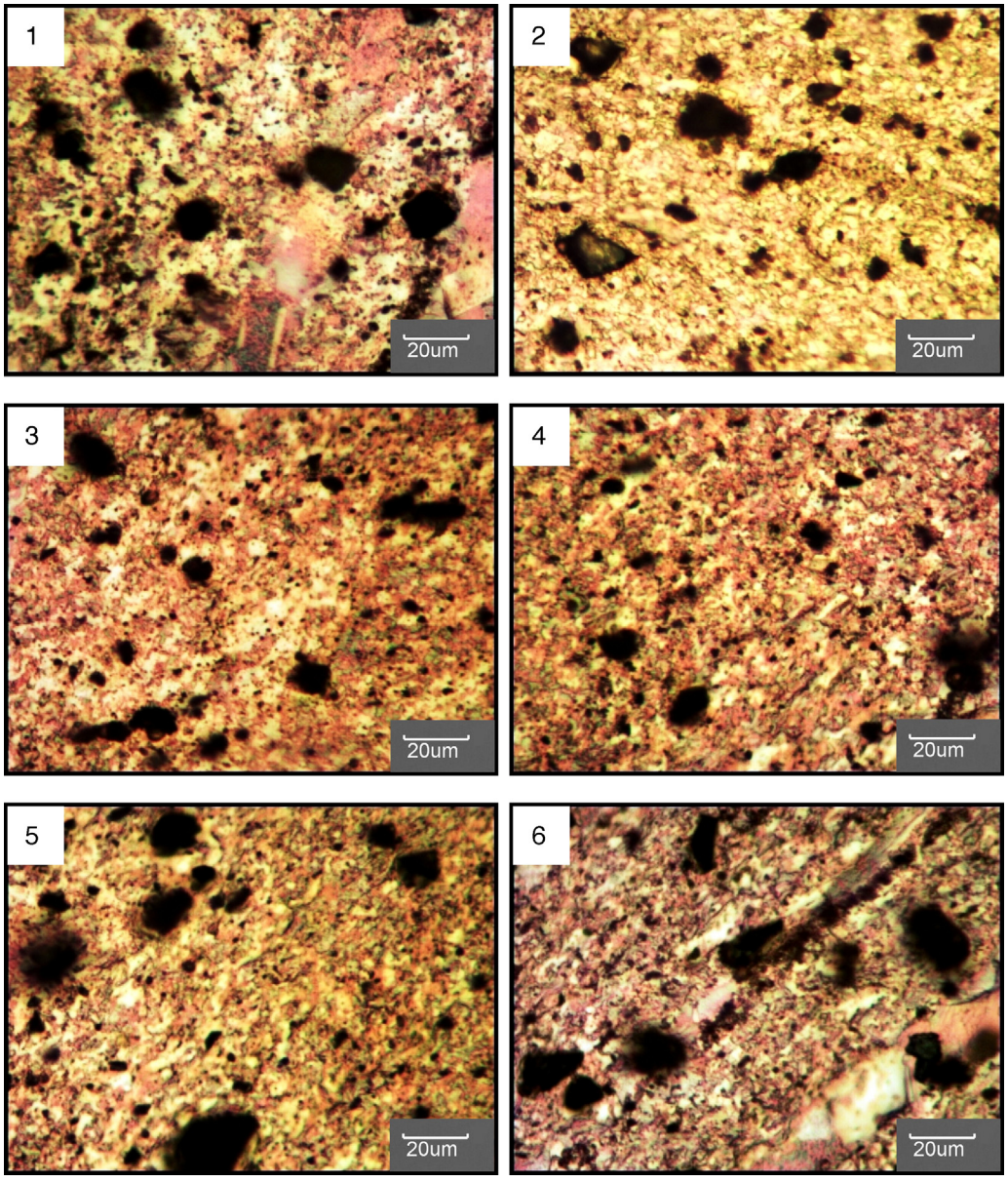

Fig. 6 – Optical photomicrograph of Cu/SiC CMC observed at various locations.

Secondly, the presence of ceramic particle plays another role. The pinning effect of the ceramic particle on the copper matrix impedes the grain growth by suppressing grain boundary sliding.

Fig. 10 presents the SEM micrographs of CMCs reinforced with various ceramic particles which clearly reveal the distribution of ceramic particles in the copper matrix. Fairly homogeneous distribution was observed. No cluster of particles is seen. Further, there is no segregation of particles along the grain boundaries. The distribution is almost intra granular. The mechanical and tribological properties of CMCs are dictated by the nature of distribution. Homogeneous and intra granular distribution is preferred to obtain superior properties. The FSP process has resulted in the desirable distribution. Liquid metallurgy routes often produce inhomogeneous and inter granular distribution due to solidification phenomena. The movement of ceramic particles within the copper matrix during processing due to density gradient is absolutely absent. This results in proper distribution. However, occurrence of ceramic particle clusters in FSP was reported in some literatures [14,15,40,41]. The FSP parameters tool rotational speed and traverse speed affect the distribution. A lower tool rotational speed and a higher traverse speed will lead to clustering and poor distribution. The fine, homogeneous distribution in this work confirms that the chosen set of process parameters is adequate to produce the desirable distribution.

FSP resulted a change in the size and morphology of ceramic particles except for Al_2O_3 particles comparing Fig. 10 and Fig. 3. The severe plastic deformation coupled with the rotating action of the tool is able to shatter the ceramic particles. The vigorous stirring action of the tool knocks off the sharp corners of the ceramic particle. Large size variation of

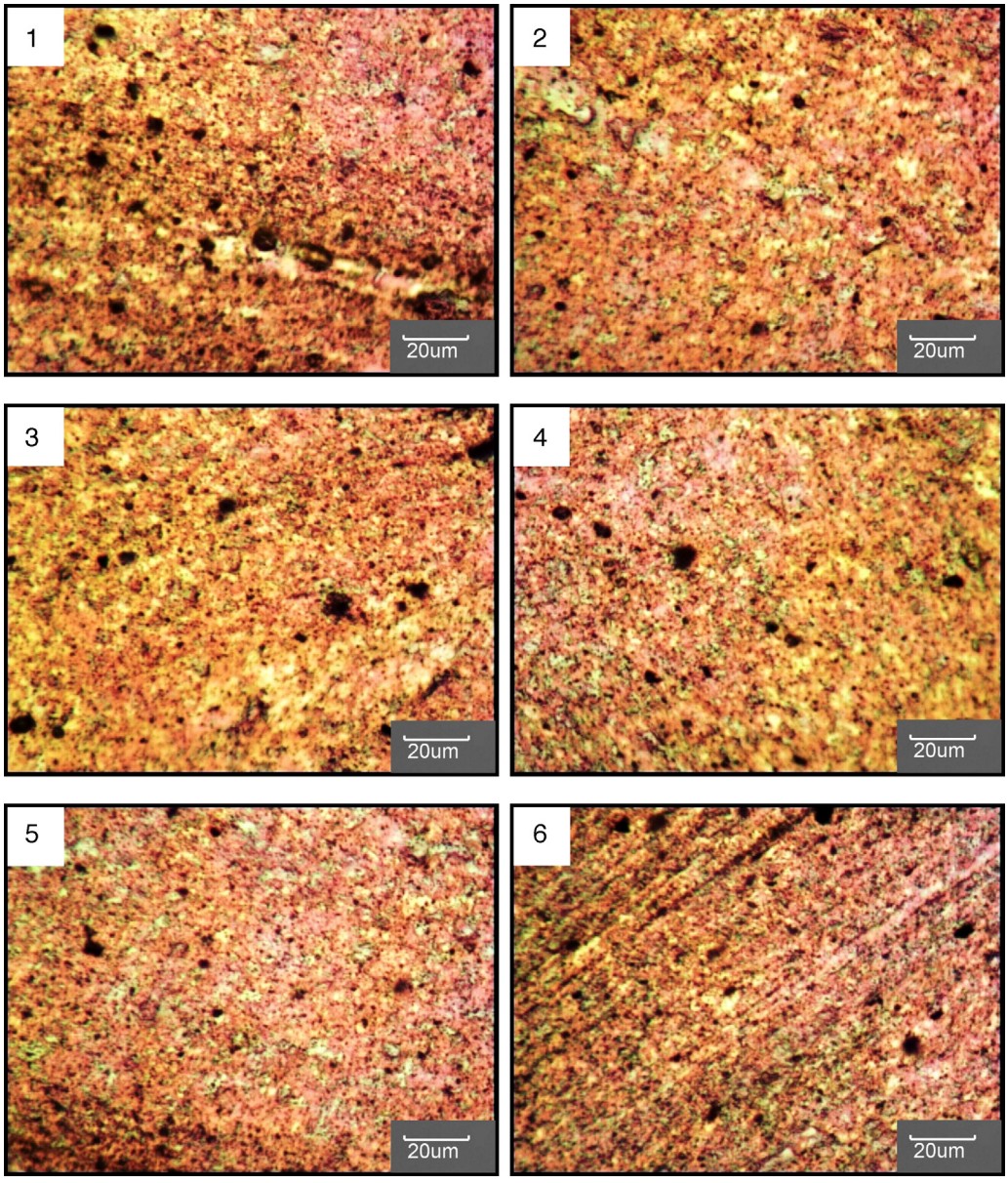

Fig. 7 – Optical photomicrograph of Cu/Al_2O_3 CMC observed at various locations.

ceramic particles (SiC, B_4C and TiC) in Fig. 10 confirms the fragmentation. Similar observations were reported by others [16,34,36]. The fragmentation depends upon the size and shape of the particles. Large size particles and irregular or polygonal shape particles have the tendency to break off during FSP. The retention of shape and size of Al_2O_3 particles in Fig. 10b after FSP, which did not undergo fragmentation confirms this statement. It is notable in Fig. 10 that the large ceramic particles are not surrounded by debris generated due to fragmentation. There is no clustering of small debris either. This suggests that the debris also mixed well with the plasticized copper and distributed homogeneously in the CMC. The size of debris is considerably low in the order of nanometer compared to the size of initially packed ceramic particles. The large size variation leads to functionally graded local areas within the CMC.

Fig. 11 depicts the SEM micrographs of CMCs reinforced with various ceramic particles at higher magnification. The etchant used in this work reveals the grain boundaries. The interface between the copper matrix and the ceramic particle is detailed in this figure. The interface is clear without the presence of pores or reaction products. Each type of ceramic particle appears to be bonded well with the copper matrix. Barmouz et al. [21] encountered a large number of pores around SiC particles in the Cu/SiC CMC fabricated using FSP technique. No such pores are observed near any ceramic particle in Fig. 11. This can be related to sufficient material flow and plasticization of copper under the chosen experimental conditions. The interface plays a crucial role in tensile loading and sliding wear to transfer the load effectively to the ceramic particle. Good interfacial bonding is a prerequisite in spite of homogeneous distribution to enhance the

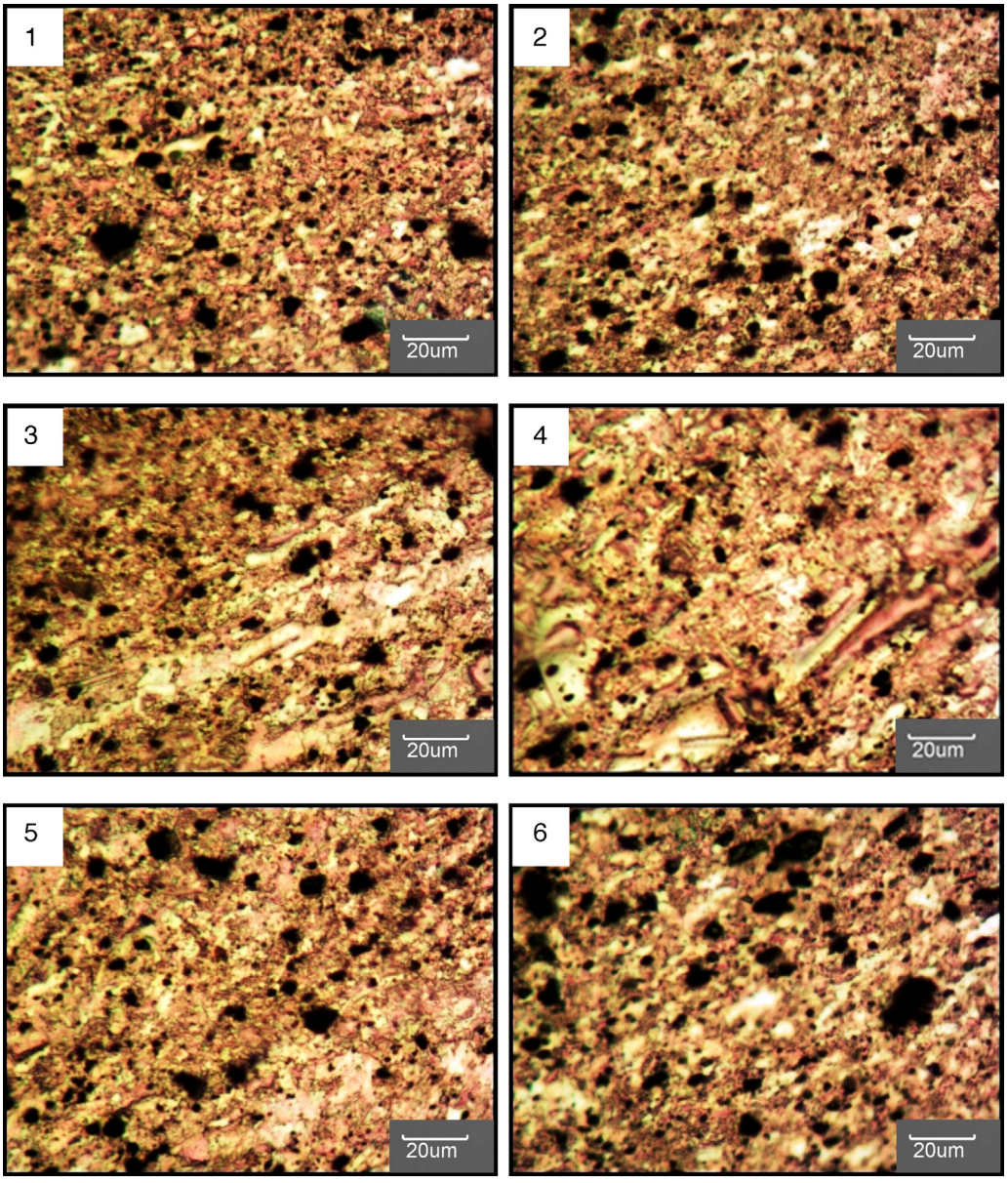

Fig. 8 – Optical photomicrograph of Cu/B_4C CMC observed at various locations.

properties. The temperature of the processing method influences the interfacial strength significantly. Higher processing temperature tends to initiate interfacial reactions between the copper matrix and the ceramic particle. The reaction products usually surround the ceramic particle and weaken the interfacial strength. Frage et al. [33] detected reaction products around B_4C particles in the Cu/B_4C composite fabricated using the liquid metallurgy route. Absence of reaction products shows that the temperature rise during FSP is insufficient to trigger any interfacial reaction.

Fig. 12 shows the EDS maps of CMCs reinforced with various ceramic particles. The element distribution of copper matrix and reinforcements are clearly visible. The reinforcement elements are dispersed all over the copper matrix. This confirms proper mixing of ceramic reinforcement particles with the copper. Further, the reinforcement elements are evenly distributed and there is no presence of element rich zones. The variation in element distribution in the figure is minimum. This validates homogeneous distribution and the absence of any interfacial reaction.

3.3. *Microhardness of CMCs*

Table 1 displays the mirohardness of CMCs reinforced with various ceramic particles. The microhardess of as received copper was 70 Hv. The reinforcement of ceramic particles increases the microhardess above 110 Hv. Cu/B_4C CMC recorded a maximum microhardness of 135 Hv. The rise in the microhardess of CMCs indicates that the ceramic particles contributed remarkably to the strengthening of the copper matrix. The hindrance to dislocation movement by higher dislocation density enhances hardness. The strengthening can be attributed to the following factors. The hardness of ceramic particles is extremely higher to that of copper matrix. The

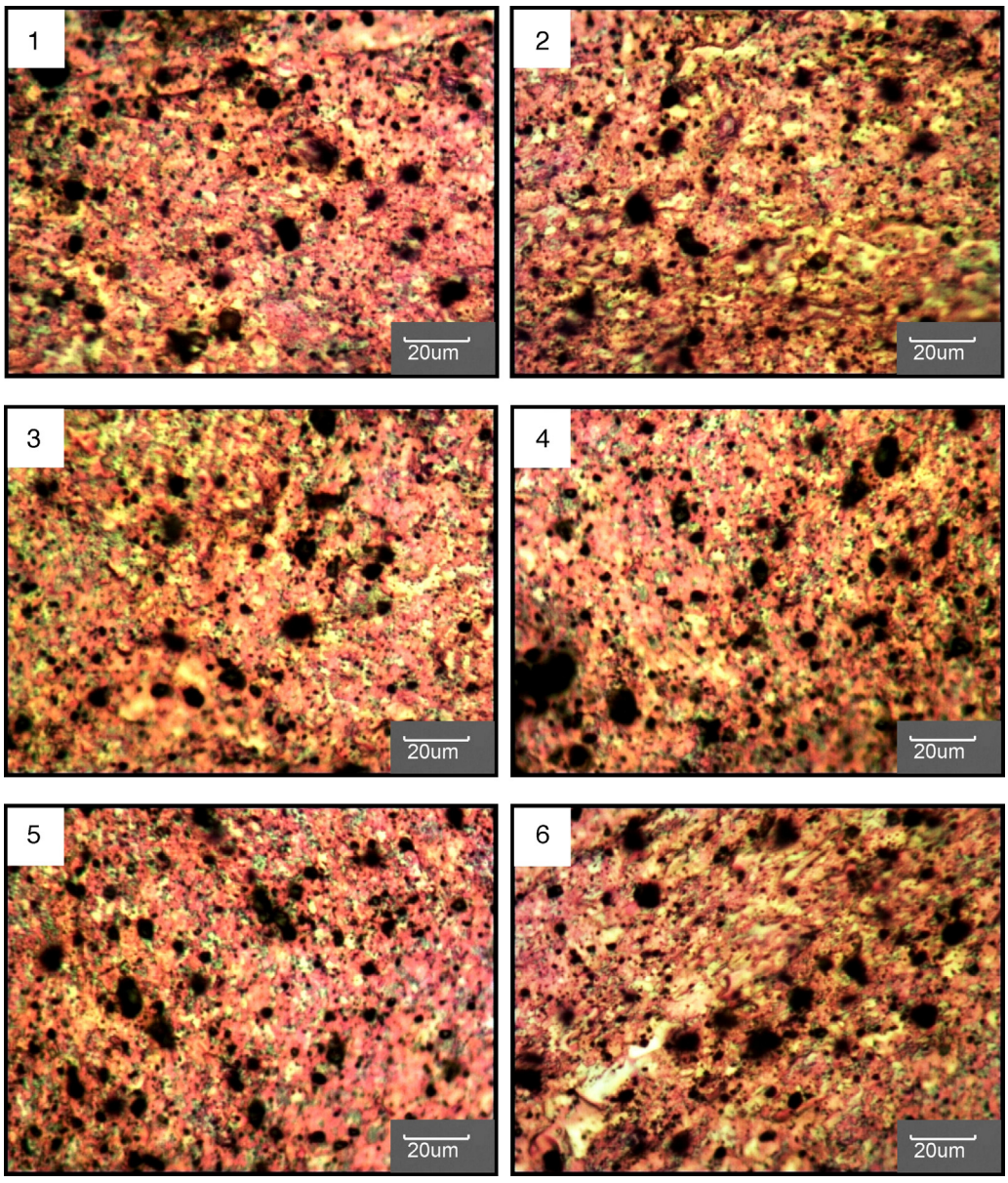

Fig. 9 – Optical photomicrograph of Cu/TiC CMC observed at various locations.

dispersion of ceramic particles as a hard phase in the copper matrix results in strengthening. According to Hall–Petch relationship, the grain size influences the mechanical properties of metallic materials. The grain size of CMCs is smaller to that of the copper matrix due to grain refinement of ceramic particle. The fine grains improve the hardness. Thirdly, the difference in thermal contraction between the copper matrix and the ceramic particles produces quench hardening effect. Further, the homogeneous distribution of ceramic particles all over the copper matrix invokes Orowan strengthening.

The hardness of Cu/B_4C CMC is found to be higher among the other CMCs produced. But the variation of hardness of various CMCs is less than 20 Hv. The mechanical properties of CMCs are generally influenced by the type, size, shape, volume fraction and spatial distribution of ceramic particles [21,24,42]. All types of ceramic particles exhibited homogeneous distribution in the copper matrix for a chosen constant volume fraction. Absence of clusters and porosity ensures minimum hardness variation. The shape variation can be considered negligible. All ceramic particles are characterized by irregular polygonal shape. None of the ceramic particle has a spherical shape to induce significant shape variation. Al_2O_3 particle is smaller in size compared to other ceramic particles studied in this work. However, it should be taken into account that other ceramic particles (SiC, B_4C and TiC) encountered fragmentation during FSP, which lead to the generation of evenly distributed fine particles. The hardness of B_4C is higher compared to SiC, Al_2O_3 and TiC, which could be the possible cause for higher hardness of Cu/B_4C CMC.

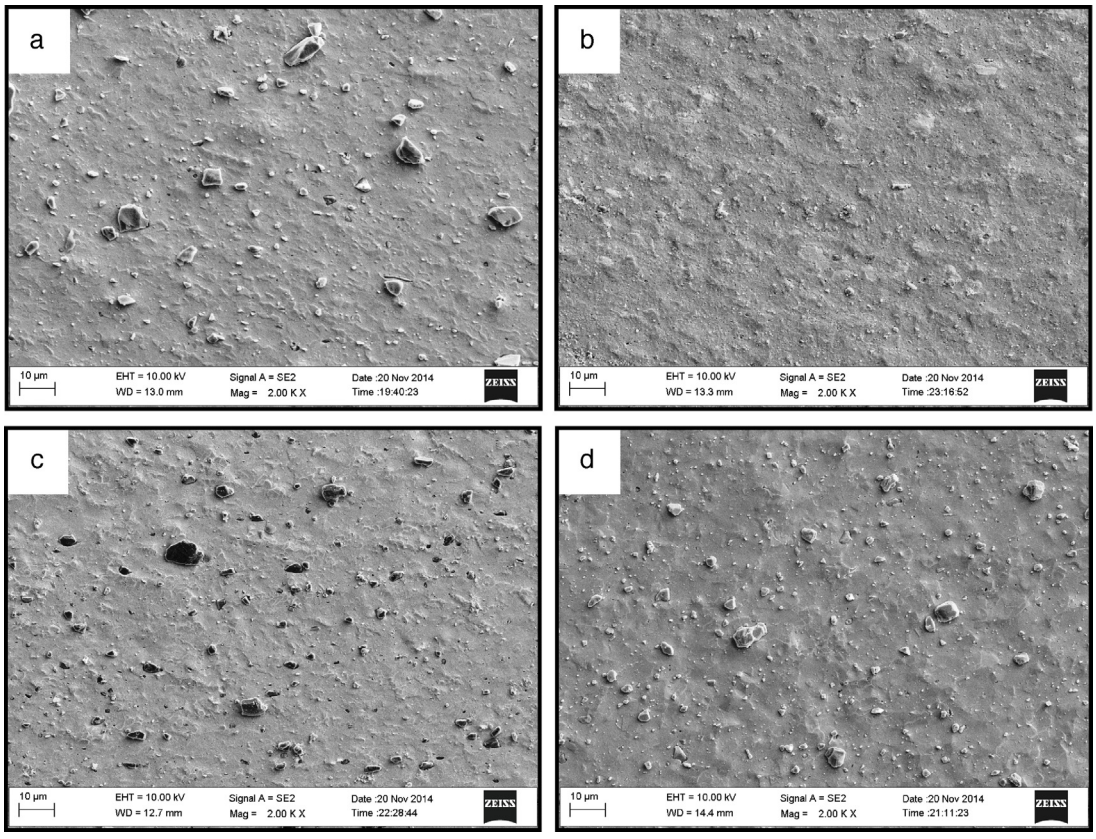

Fig. 10 – FESEM micrograph CMCs reinforced with: (a) SiC, (b) Al_2O_3, (c) B_4C and (d) TiC.

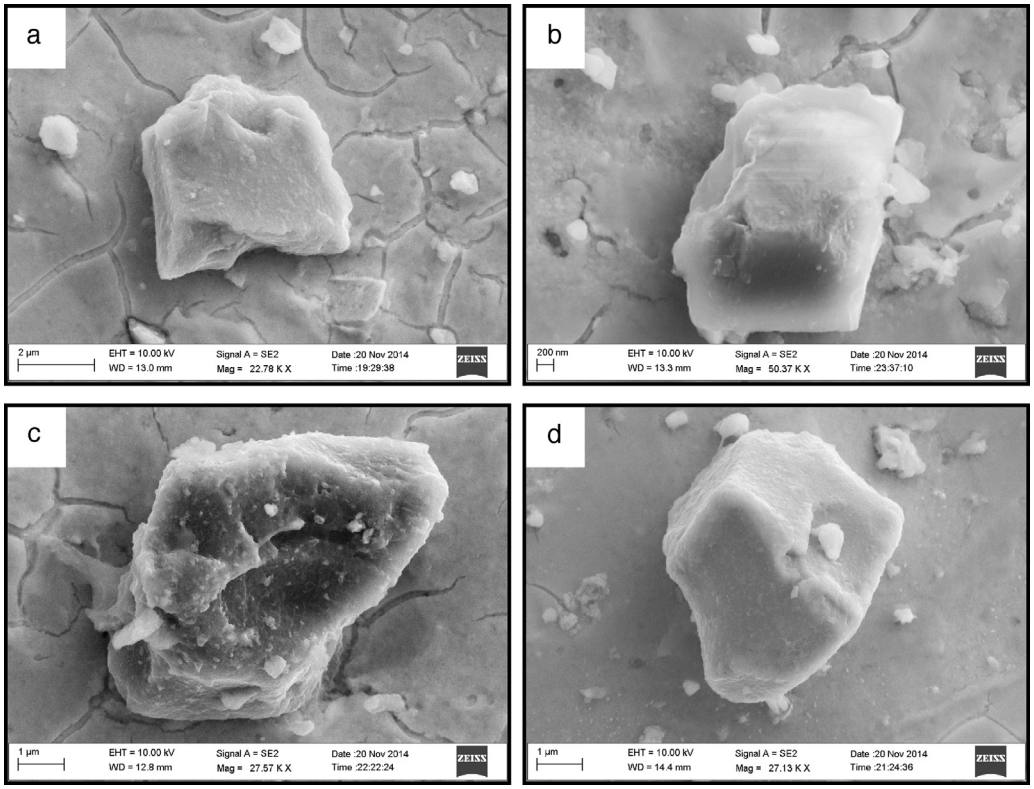

Fig. 11 – FESEM micrograph CMCs reinforced with: (a) SiC, (b) Al_2O_3, (c) B_4C and (d) TiC at higher magnification.

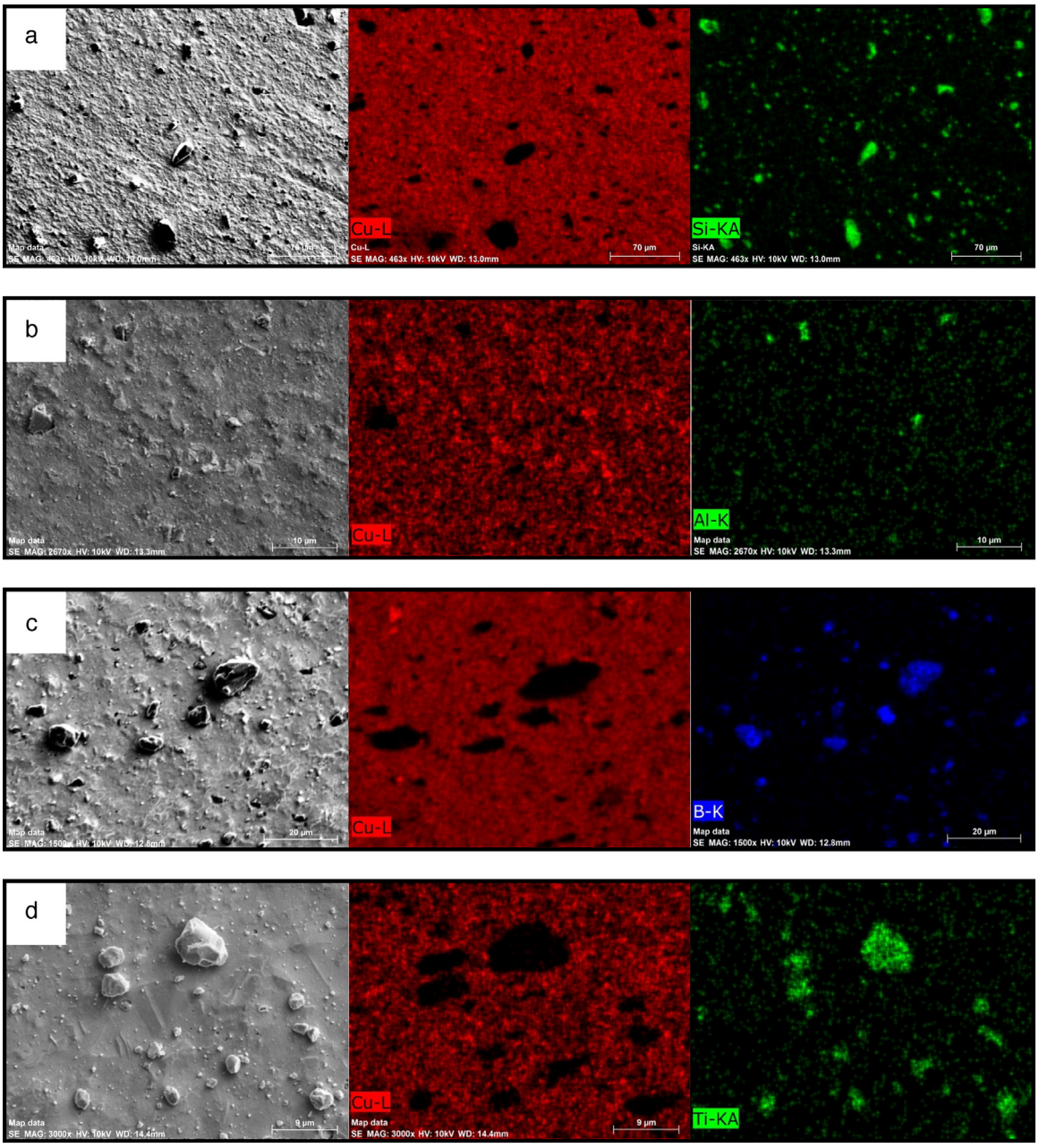

Fig. 12 – EDS maps of CMCs reinforced with: (a) SiC, (b) Al_2O_3, (c) B_4C and (d) TiC.

3.4. *Sliding wear behavior of CMCs*

Table 1 presents the wear rate of CMCs reinforced with various ceramic particles. The wear rate of copper matrix is 385×10^{-5} mm^3/m. The incorporation of ceramic particles reduces the wear rate below 250×10^{-5} mm^3/m. Cu/B_4C CMC exhibited a lowest wear rate of 213×10^{-5} mm^3/m. The results indicate that the addition of ceramic particles considerably improved the wear resistance of the CMCs. The reduction in wear rate can be explained as follows. The volume loss of material due to sliding wear is given by the following expression [43]:

$$\text{Volume loss} = \frac{\text{Wear coefficient} \times \text{Applied load} \times \text{Sliding distance}}{\text{Hardness of material}} \quad (1)$$

According to this expression, volume loss is inversely proportional to the hardness of the sliding material. Higher the hardness of the material, lower will be the wear rate. The enhancement of hardness due to fine distribution of ceramic particles and grain refinement is the primary cause for enhancement of wear resistance. The contact area between the CMC and the counter disk is reduced in comparison to unreinforced copper due to the presence of ceramic particles which bear the applied normal load. The good interfacial bonding between the copper matrix and the ceramic particle retards the detachment of ceramic particle from the copper matrix during sliding. The aforementioned factors lead to higher wear resistance of CMCs.

Fig. 13 displays the worn surface of CMCs reinforced with various ceramic particles. The worn surface of pure copper

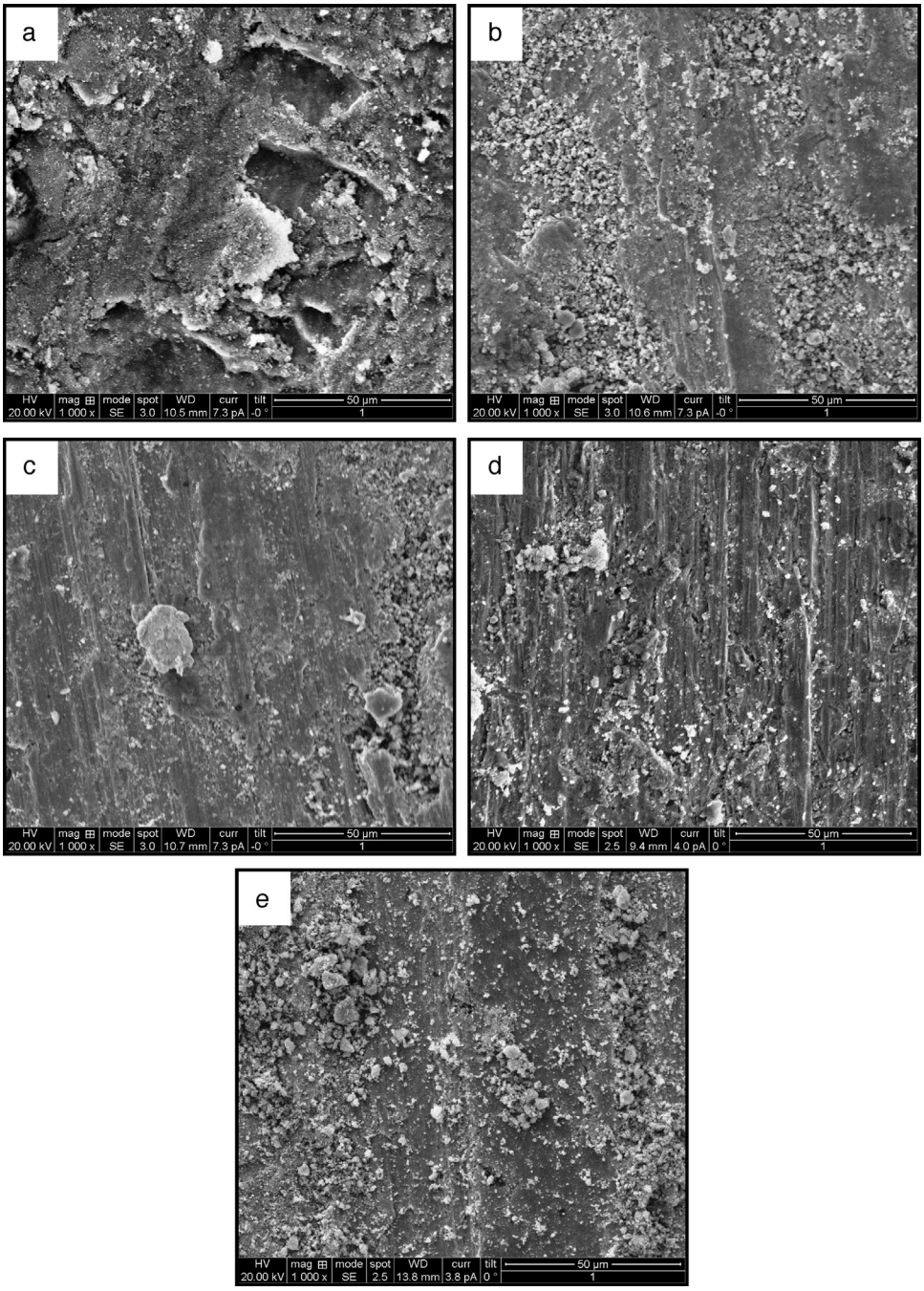

Fig. 13 – FESEM micrograph of worn surface of: (a) pure copper and CMCs reinforced with: (b) SiC, (c) Al_2O_3, (d) B_4C and (e) TiC.

in Fig. 13a shows large amount of plastic deformation and deep craters. These are prominent characteristics of adhesive wear. In the absence of ceramic particles, the copper pin surface is in direct contact with the counterface. The asperities of the copper pin and the counter disk are deformed during sliding wear and solid state joint is created. This causes sliding difficult increasing wear loss. The cyclic deformation hardens the area near the adhesion region leading to the generation of micro cracks and cavities. These micro cracks coalescence and eventually detach the surface layer intensifying the adhesive wear. Hence, adhesive wear is the reason for high wear loss of pure copper. The worn surface of the CMCs in Fig. 13b–e presents roughly a uniform flat surface. The variation in worn surface morphology of various CMCs is insignificant. Little plastic deformation is evident on the worn surface. The ceramic particles restrict the free flow of softened copper due to friction during sliding wear. The worn surfaces are covered with numerous wear debris. The wear mode is changed to abrasive wear.

Fig. 14 displays the wear debris of CMCs reinforced with various ceramic particles. The wear debris of pure copper in Fig. 14a shows large size debris as well as small debris. The

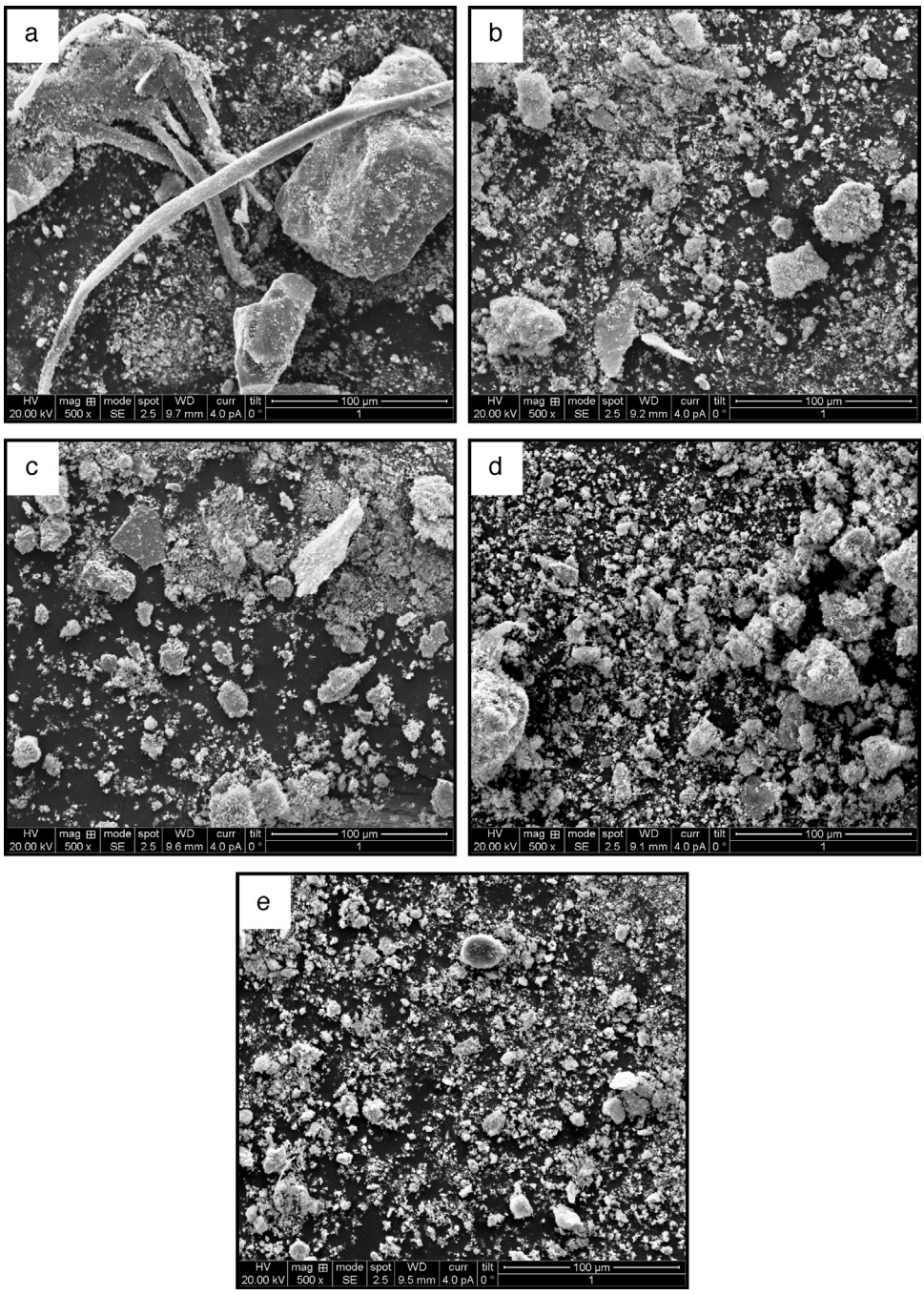

Fig. 14 – FESEM micrograph of wear debris of: (a) pure copper and CMCs reinforced with: (b) SiC, (c) Al_2O_3, (d) B_4C and (e) TiC.

size and morphology of the debris are directly influenced by the wear mechanism. Large size debris confirms that the wear mechanism of pure copper is prominently adhesion. The worn surface of the CMCs in Fig. 13b–e presents fine size spherical shape particles. This suggests that the addition of ceramic particles influenced the wear mechanism. The difference in wear debris size and morphology of various CMCs is trivial. The generation of fine debris during the wear process can be attributed to the following causes; (a) the increase in hardness of the CMCs compared to copper and (b) the reduced probability of the sliding pin and the counterface disk due to the incorporation of ceramic particles. The ceramic particles are detached from the copper matrix as sliding wear progresses. These detached particles alter two body abrasion wear into three body abrasion wear. The latter produces fine size wear debris. The debris particles lying on the wear track are repeatedly subjected to crushing action between the sliding pin and the counter surface due to the applied load. The wear process becomes analogous to high energy ball milling resulting in finer debris.

4. Conclusion

Cu/X (X = SiC, Al_2O_3, B_4C and TiC) CMCs were successfully synthesized using FSP. The microstructure, microhardness and sliding wear behavior were evaluated. The following conclusions are derived from the present work.

- The variation in the stir zone, grain size, microhardness and wear rate was within a short range. Nevertheless, Cu/B_4C CMC showed superior hardness and wear resistance compared to other CMCs produced in this work under the same set of experimental conditions.
- The distribution of the ceramic particles in the CMCs was independent of the location in the stir zone. The distribution was homogeneous and unaffected by the type of ceramic particle used.
- SiC, B_4C and TiC particles encountered fragmentation during FSP due to severe plastic deformation and interaction with the rotating tool. The fragmented debris also mixed well with the plasticized copper and distributed homogeneously in the CMC. Al_2O_3 particle did not suffer fragmentation due to its smaller size.
- There was no interfacial reaction between copper and any type of ceramic particle and good interfacial bonding was observed.
- All types of ceramic particles enhanced the wear resistance of pure copper and affected the wear mechanism. The wear mode changed from adhesion to abrasion. The plastic deformation on the worn surface disappeared with the addition of ceramic particles. The wear debris became finer in size.
- FSP is a suitable processing method to produce CMCs reinforced with any kind of ceramic particles with acceptable properties.

Conflicts of interest

The authors declare no conflicts of interest.

Acknowledgement

The authors are grateful to the Management and Department of Mechanical Engineering, Coimbatore Institute of Technology, Coimbatore, India for extending the facilities to carry out this investigation. The authors are also thankful to Dr. S.J. Vijay and Mr. I. Devamanoharan for their assistance.

REFERENCES

[1] Surekha K, Els-Botes A. Development of high strength, high conductivity copper by friction stir processing. Mater Des 2011;32(2):911–6.
[2] Rajkumar K, Aravindan S. Tribological performance of microwave sintered copper–TiC–graphite hybrid composites. Tribol Int 2011;44(4):347–58.
[3] Dhokey NB, Paretkar RK. Study of wear mechanisms in copper-based SiC_p (20% by volume) reinforced composite. Wear 2008;265(1–2):117–33.
[4] Sapate SG, Uttarwar A, Rathod RC, Paretkar RK. Analyzing dry sliding wear behaviour of copper matrix composites reinforced with pre-coated SiC_p particles. Mater Des 2009;30(2):376–86.
[5] Romankova S, Hayasakab Y, Shchetinin IV, Yoona JM, Komarov SV. Fabrication of Cu–SiC surface composite under ball collisions. Appl Surf Sci 2011;257(11):5032–6.
[6] Wei X, Rui H, Shan LJ, Zhi FH. Effect of electrical current on tribological property of Cu matrix composite reinforced by carbon nanotubes. Trans Nonferrous Met Soc China 2011;21(10):2237–41.
[7] Kim JH, Yun JH, Park YH, Cho KM, Choi ID, Park IM. Manufacturing of Cu–TiB_2 composites by turbulent in situ mixing process. Mater Sci Eng A 2007;449–451:1018–21.
[8] Xing H, Cao X, Hu W, Zhao L, Zhang J. Interfacial reactions in 3D-SiC network reinforced Cu-matrix composites prepared by squeeze casting. Mater Lett 2005;59(12):1563–6.
[9] Ramesh CS, Ahmed RN, Mujeebu MA, Abdullah MZ. Development and performance analysis of novel cast copper–SiC–Gr hybrid composites. Mater Des 2009;30(6):1957–65.
[10] Arora HS, Singh H, Dhindaw BK. Composite fabrication using friction stir processing—a review. Int J Adv Manuf Technol 2012;61(9–12):1043–55.
[11] Ma ZY. Friction stir processing technology: a review. Metall Mater Trans A 2008;39(3):642–58.
[12] Mishra RS, Ma ZY, Charit I. Friction stir processing: a novel technique for fabrication of surface composite. Mater Sci Eng A 2003;341(1–2):307–10.
[13] Lee CJ, Huang JC, Hsieh PJ. Mg based nano-composites fabricated by friction stir processing. Scr Mater 2006;54(7):1415–20.
[14] Yang M, Xu C, Wu C, Lin K, Chao YJ, An L. Fabrication of AA6061/Al_2O_3 nano ceramic particle reinforced composite coating by using friction stir processing. J Mater Sci 2010;45(16):4431–8.
[15] Aruri D, Adepu K, Adepu K, Bazavada K. Wear and mechanical properties of 6061-T6 aluminum alloy surface hybrid composites [(SiC + Gr) and (SiC + Al_2O_3)] fabricated by friction stir processing. J Mater Res Technol 2013;2(4):362–9.
[16] Azizieh M, Kokabi AH, Abachi P. Effect of rotational speed and probe profile on microstructure and hardness of AZ31/Al_2O_3 nanocomposites fabricated by friction stir processing. Mater Des 2011;32(4):2034–41.
[17] Sathiskumar R, Murugan N, Dinaharan I, Vijay SJ. Fabrication and characterization of Cu/B_4C surface dispersion strengthened composite using friction stir processing. Arch Metall Mater 2014;59(1):83–7.
[18] Kahrizsangi AG, Bozorg SFK. Microstructure and mechanical properties of steel/TiC nano-composite surface layer produced by friction stir processing. Surf Coat Technol 2012;209:15–22.
[19] Shamsipura A, Bozorg SFK, Hanzakia AZ. The effects of friction-stir process parameters on the fabrication of Ti/SiC nano-composite surface layer. Surf Coat Technol 2011;206(16):1372–81.
[20] Barmouz M, Givi MKB, Seyfi J. On the role of processing parameters in producing Cu/SiC metal matrix composites via friction stir processing: Investigating microstructure, microhardness, wear and tensile behavior. Mater Charact 2011;62(1):108–17.
[21] Barmouz M, Asadi P, Givi MKB, Taherishargh M. Investigation of mechanical properties of Cu/SiC composite fabricated by FSP: effect of SiC particles size and volume fraction. Mater Sci Eng A 2011;528(3):1740–9.

[22] Barmouz M, Givi MKB. Fabrication of in situ Cu/SiC composites using multi-pass friction stir processing: evaluation of microstructural, porosity, mechanical and electrical behavior. Compos Part A 2011;42(10):1445–53.
[23] Sarmadi H, Kokabi AH, Reihani SMS. Friction and wear performance of copper–graphite surface composites fabricated by friction stir processing (FSP). Wear 2013;304(1–2):1–12.
[24] Sathiskumar R, Murugan N, Dinaharan I, Vijay SJ. Characterization of boron carbide particulate reinforced in situ copper surface composites synthesized using friction stir processing. Mater Charact 2013;84:16–27.
[25] Sathiskumar R, Murugan N, Dinaharan I, Vijay SJ. Prediction of mechanical and wear properties of copper surface composites fabricated using friction stir processing. Mater Des 2014;55:224–34.
[26] Akramifard HR, Shamanian M, Sabbaghian M, Esmailzadeh M. Microstructure and mechanical properties of Cu/SiC metal matrix composite fabricated via friction stir processing. Mater Des 2014;54:838–44.
[27] Fenoel MNA, Simar A, Shabadi R, Taillard R, Meester BD. Characterization of oxide dispersion strengthened copper based materials developed by friction stir processing. Mater Des 2014;60:343–57.
[28] Khosravi J, Givi MKB, Barmouz M, Rahi A. Microstructural, mechanical, and thermophysical characterization of Cu/WC composite layers fabricated via friction stir processing. Int J Adv Manuf Technol 2014;74(5–8):1087–96.
[29] Sabbaghian M, Shamanian M, Akramifard HR, Esmailzadeh M. Effect of friction stir processing on the microstructure and mechanical properties of Cu–TiC composite. Ceram Int 2014;40(8):12969–76.
[30] Raju LS, Kumar A. Influence of Al_2O_3 particles on the microstructure and mechanical properties of copper surface composites fabricated by friction stir processing. Defence Technol 2014;10(4):375–83.
[31] Romankov S, Hayasaka Y, Shchetinin IV, Yoona JM, Komarov SV. Fabrication of Cu–SiC surface composite under ball collisions. Appl Surf Sci 2011;257(11):5032–6.
[32] Akhtar F, Askari SJ, Shah KA, Du X, Guo S. Microstructure, mechanical properties, electrical conductivity and wear behavior of high volume TiC reinforced Cu-matrix composites. Mater Charact 2009;60(4):327–36.
[33] Frage N, Froumin N, Aizenshtein M, Dariel MP. Interface reaction in the B_4C/(Cu–Si) system. Acta Mater 2004;52(9):2625–35.
[34] Minak G, Ceschini L, Boromei I, Ponte M. Fatigue properties of friction stir welded particulate reinforced aluminium matrix composites. Int J Fatigue 2009;32(1):218–26.
[35] Guo JF, Gougeon P, Chen XG. Characterisation of welded joints produced by FSW in AA 1100-B_4C metal matrix composites. Sci Technol Weld Joining 2012;17(2):85–91.
[36] Prater T. Solid-state joining of metal matrix composites: a survey of challenges and potential solutions. Mater Manuf Process 2011;26(4):636–48.
[37] Uzun H. Friction stir welding of SiC particulate reinforced AA2124 aluminium alloy matrix composite. Mater Des 2007;28(5):1440–6.
[38] Mahmoud ERI, Ikeuchi K, Takahashi M. Fabrication of SiC particle reinforced composite on aluminium surface by friction stir processing. Sci Technol Weld Joining 2008;13(7):607–18.
[39] Lim DK, Shibayanagi T, Gerlich AP. Synthesis of multi-walled CNT reinforced aluminium alloy composite via friction stir processing. Mater Sci Eng A 2009;507:194–9.
[40] Faraji G, Asadi P. Characterization of AZ91/alumina nanocomposite produced by FSP. Mater Sci Eng A 2011;528:2431–40.
[41] Sathiskumar R, Murugan N, Dinaharan I, Vijay SJ. Effect of traverse speed on microstructure and microhardness of Cu/B_4C surface composite produced by friction stir processing. Trans Indian Inst Met 2013;66:333–7.
[42] Sannino AP, Rack HJ. Dry sliding wear of discontinuously reinforced aluminum composites: review and discussion. Wear 1995;189:1–19.
[43] Kumar S, Sarma VS, Murty BS. Influence of in situ formed TiB_2 particles on the abrasive wear behaviour of Al–4Cu alloy. Mater Sci Eng A 2007;465(1–2):160–4.